

**Dressed Polyakov loop and phase diagram of hot quark matter in a magnetic field**Raoul Gatto<sup>1,\*</sup> and Marco Ruggieri<sup>2,†</sup><sup>1</sup>*Département de Physique Théorique, Université de Genève, CH-1211 Genève 4, Switzerland*<sup>2</sup>*Yukawa Institute for Theoretical Physics, Kyoto University, Kyoto 606-8502, Japan*

(Received 11 July 2010; published 23 September 2010)

We evaluate the dressed Polyakov loop for hot quark matter in strong magnetic field. To compute the finite temperature effective potential, we use the Polyakov extended Nambu–Jona-Lasinio model with eight-quark interactions taken into account. The bare quark mass is adjusted in order to reproduce the physical value of the vacuum pion mass. Our results show that the dressed Polyakov loop is very sensitive to the strength of the magnetic field, and it is capable to capture both the deconfinement crossover and the chiral crossover. Additionally, we self-consistently compute the phase diagram of the model. We find a tiny split of the two aforementioned crossovers as the strength of the magnetic field is increased. Concretely, for the largest value of magnetic field investigated here,  $eB = 19m_\pi^2$ , the split is of the order of 10%. A qualitative comparison with other effective models and recent lattice results is also performed.

DOI: 10.1103/PhysRevD.82.054027

PACS numbers: 12.38.Aw, 12.38.Mh

**I. INTRODUCTION**

The nature of the Quantum Chromodynamics (QCD) vacuum is one of the most intriguing aspects of modern physics. Additionally, it is very hard to get a full understanding of its properties, because its most important characteristics, namely, chiral symmetry breaking and color confinement, have a nonperturbative origin, and the use of perturbative methods is useless. One of the best strategies to overcome this problem is offered by lattice QCD simulations at zero chemical potential (see [1–4] for several examples and see also references therein). At vanishing quark chemical potential, it is almost established that two crossovers take place at nearly the same temperature: one for quark deconfinement, and another one for the (approximate) restoration of chiral symmetry. It is still under debate whether two crossovers should occur at exactly the same temperature; see, for example, the report in [2].

An alternative approach to the physics of strong interactions, which is capable of capturing some of the non-perturbative properties of the QCD vacuum while at the same time being easy to manage mathematically, is the Nambu–Jona-Lasinio (NJL) model [5] (see also [6] for reviews). In this model, the QCD gluon-mediated interactions are replaced by effective interactions among quarks, which are built in order to respect the global symmetries of QCD. Since dynamical gluons are absent in this model, it is not a gauge theory. However, it shares the global symmetries of the QCD action; moreover, the parameters of the NJL model are fixed to reproduce some phenomenological quantity of the QCD vacuum: in its simplest version, the pion decay constant, the vacuum pion mass, and the vacuum chiral condensate are reproduced. Therefore, it is

reasonable that the main characteristics of its phase diagram represent, at least qualitatively, those of QCD.

Critically speaking, the worst aspect of the NJL model is that it lacks confinement: massive quark poles of the quark propagator are present at any temperature and/or chemical potential. It is well known that color confinement can be described in terms of the center symmetry of the color gauge group and of the Polyakov loop [7], which is an order parameter for the center symmetry. Motivated by this property, the Polyakov extended Nambu–Jona-Lasinio model (P-NJL model) has been introduced [8,9], in which the concept of statistical confinement replaces that of the true confinement of QCD, and an effective interaction among the chiral condensate and the Polyakov loop is achieved by a covariant coupling of quarks with a background temporal gluon field. In the literature, there are several studies about various aspects of the P-NJL model. Its phase structure with two flavors and symmetric quark matter has been investigated in [10–13]; a P-NJL model with a Van der Monde term has been considered in [14]; phase structure with 2 + 1 flavors has been studied in [15]; possible realization of the quarkyonic phase [16] has been discussed in [15,17]; mass dependence of the phase diagram, and a possible emergence of the quarkyonic phase, is investigated in [18]; phase diagram with imaginary chemical potential has been studied in [19,20]; dual quark condensate has been computed in [21]; neutral phases have been investigated in [22]; phase diagram with asymmetric quark matter have been studied in [23]; nonlocal extension has been introduced in [24]; role of eight-quark interactions in the P-NJL context has been elucidated in [25].

The modification of the QCD vacuum—and of its thermal excitations as well—under the influence of external fields is an attractive topic. Firstly, it is extremely interesting to understand how an external field can modify the main characteristics of confinement and spontaneous chiral symmetry breaking. Lattice studies on the response to

\*raoul.gatto@unige.ch

†ruggieri@yukawa.kyoto-u.ac.jp

external magnetic fields can be found in [26–28]. QCD in chromomagnetic fields has been investigated on the lattice in [29,30]. Previous studies of QCD in magnetic fields, and of QCD-like theories as well, can be found in [31–34]. Self-consistent model calculations of magnetic catalysis and of deconfinement pseudocritical temperature in magnetic field have been performed firstly in [35] within the P-NJL model, and then in [36] using the Polyakov extended quark-meson model. Effective models in chromomagnetic fields have been considered in [37]. Additionally, strong magnetic fields with order of magnitude between  $eB \approx m_\pi^2$  and  $eB \approx 15m_\pi^2$  might be produced in the very first moments of the noncentral heavy ion collisions [38,39]. In this case, it has been argued that the nontrivial topological structure of thermal QCD gives rise to the chiral magnetic effect (CME) [38,40,41].

Beside the Polyakov loop, it has been suggested [42] that another observable which is an order parameter for the center symmetry, and hence for confinement, is the dressed Polyakov loop. From the mathematical point of view, the dressed Polyakov loop is built from the canonical (called *thin*) Polyakov loop, by dressing it with higher order loops, which wind once around the compact temporal direction. In this context, the order of a loop is given by its length; the thin Polyakov loop corresponds to the shortest one. The dressing becomes more important when quark masses are finite (the Polyakov loop is an exact order parameter for confinement-deconfinement only in the ideal case of static quarks with infinite masses). In [43], the dressed Polyakov loop has been computed within the scheme of truncated Schwinger-Dyson equations, with a model for resummed quark-gluon vertex and in-medium gluon propagator computed on the lattice. Within the NJL model, in which the QCD interaction among quarks is replaced by a contact four-fermion interaction,  $\Sigma_1$  has been computed at finite temperature and chemical potential in [44]. Finally, the dressed Polyakov loop has been computed within the P-NJL model in [21] at finite temperature.

In this article, we compute the phase structure and the dressed Polyakov loop of hot massive two-flavor quark matter at zero chemical potential in an external magnetic field. To compute the effective potential, we rely on the P-NJL model of strongly interacting quarks. We will limit ourselves to the one-loop approximation (saddle point), which is enough to draw a phase structure. The novelty of the present article is manifold. Firstly, we introduce the eight-quark interaction [45–48] in the P-NJL model in an external magnetic field (previous studies of the P-NJL model in magnetic and chromomagnetic fields neglected this kind of interaction). Within the NJL model, it has been shown that the eight-quark interactions naturally lower the pseudocritical temperature for (approximate) chiral symmetry restoration. Magnetic catalysis in the NJL model with multi-quark interactions has been investigated in [48]. However, in those studies, the computation of quantities

relevant for deconfinement crossover is lacking. On the other hand, in [25], the P-NJL model with multi-quark interaction has been investigated, but without magnetic field. It is of interest, then, to study the response of quark matter to magnetic fields in the framework of the P-NJL model with eight-quark interaction. In doing this, we will consider quarks with finite values of bare mass, fixed to reproduce the vacuum pion mass, while in a previous study [35] this problem was studied only in the chiral limit.

Moreover, we compute the dressed Polyakov loop,  $\Sigma_1$ , in a magnetic field. Along this line, we anticipate one of our results, namely, that the dressed Polyakov loop,  $\Sigma_1$ , is capable of feeling both the Polyakov loop and the chiral condensate crossovers, whatever the strength of the magnetic field is. This occurs despite the tiny split of the two crossovers, which we observe at sufficiently strong magnetic field strength. Therefore, in view of an effective theory for finite temperature QCD in terms of just one order parameter, our results are encouraging.

The plan of the paper is as follows. In Sec. II, we present the model we use. In Sec. III, we show and discuss our numerical results. Finally, in Sec. IV, we draw our conclusions.

## II. DRESSED POLYAKOV LOOP IN THE EFFECTIVE MODEL

In this article, we model two-flavor quark matter by the following Lagrangian density:

$$\begin{aligned} \mathcal{L} = & \bar{q}(i\gamma^\mu D_\mu - m_0)q + g_\sigma[(\bar{q}q)^2 + (\bar{q}i\gamma_5\boldsymbol{\tau}q)^2] \\ & + g_8[(\bar{q}q)^2 + (\bar{q}i\gamma_5\boldsymbol{\tau}q)^2]^2, \end{aligned} \quad (1)$$

which corresponds to the NJL Lagrangian with multi-quark interactions [45]. The covariant derivative embeds the quark coupling to the external magnetic field and to the background gluon field as well. In Eq. (1),  $q$  represents a quark field in the fundamental representation of color and flavor (indices are suppressed for notational simplicity);  $\boldsymbol{\tau}$  is a vector of Pauli matrices in flavor space;  $m_0$  is the bare quark mass, which is fixed to reproduce the pion mass  $m_\pi = 139$  MeV in the vacuum. Our interaction in Eq. (1) consists of a four-quark term, whose coupling  $g_\sigma$  has inverse mass dimension two, and an eight-quark term, whose coupling constant  $g_8$  has inverse mass dimension eight.

The evaluation of the bulk thermodynamic quantities requires that we compute the quantum effective action of the model. This cannot be done exactly. Hence, we rely upon the one-loop approximation for the partition function, which amounts to taking the classical contribution plus the fermion determinant. In order to couple the Polyakov loop to the quark fields, it is customary, in the P-NJL model, to introduce a background temporal, static, and homogeneous Euclidean gluon field,  $A_4$ , in terms of which the Polyakov loop is given by

$$P = \frac{1}{3} \mathcal{P} \exp\left(i \int_0^\beta A_4 d\tau\right). \quad (2)$$

Here,  $\beta = 1/T$ , and  $T$  corresponds to the temperature of the bath in which the system lives.  $A_4$  is coupled to the quarks via the covariant derivative [see Eq. (1)]; as a consequence, a coupling among the quark fields and the Polyakov loop arises naturally when the integration over fermion fields in the partition function is performed.

We work in the Landau gauge, and take the magnetic field to be homogeneous, static, and aligned with the positive  $z$  axis. The one-loop thermodynamic potential of quark matter in external fields has been discussed in [35,37], in the case of canonical antiperiodic boundary conditions; following [21], it is easy to generalize it to the more general case of twisted boundary conditions:

$$\begin{aligned} \Omega = & \mathcal{U}(P, \bar{P}, T) + \frac{\sigma^2}{g_\sigma} + \frac{3\sigma^4 g_8}{g_\sigma^4} - \sum_{f=u,d} \frac{|q_f e B|}{2\pi} \sum_k \alpha_k \int_{-\infty}^{+\infty} \frac{dp_z}{2\pi} g_\Lambda(p_z, k) \omega_k(p_z) \\ & - T \sum_{f=u,d} \frac{|q_f e B|}{2\pi} \sum_k \alpha_k \int_{-\infty}^{+\infty} \frac{dp_z}{2\pi} \log(1 + 3P e^{-\beta \mathcal{E}_-} + 3\bar{P} e^{-2\beta \mathcal{E}_-} + e^{-3\beta \mathcal{E}_-}) \\ & - T \sum_{f=u,d} \frac{|q_f e B|}{2\pi} \sum_k \alpha_k \int_{-\infty}^{+\infty} \frac{dp_z}{2\pi} \log(1 + 3\bar{P} e^{-\beta \mathcal{E}_+} + 3P e^{-2\beta \mathcal{E}_+} + e^{-3\beta \mathcal{E}_+}). \end{aligned} \quad (3)$$

In the previous equation,  $\sigma = g_\sigma \langle \bar{q} q \rangle = 2g_\sigma \langle \bar{u} u \rangle$ ;  $k$  is a non-negative integer which labels the Landau level;  $\alpha_k = \delta_{k0} + 2(1 - \delta_{k0})$  counts the degeneracy of the  $k$ th Landau level. We have put

$$\omega_k(p_z)^2 = p_z^2 + 2|q_f e B|k + M^2, \quad (4)$$

with  $M = m_0 - 2\sigma - 4\sigma^3 g_8/g_\sigma^3$ . The arguments of the thermal exponentials are defined as

$$\mathcal{E}_\pm = \omega_k(p_z) \pm \frac{i(\varphi - \pi)}{\beta}, \quad (5)$$

with  $\varphi$  defined in Eq. (10).

The vacuum part of the thermodynamic potential,  $\Omega(T=0)$ , is ultraviolet divergent. This divergence is transmitted to the self-consistent equations which determine the chiral condensate and the expectation value of the Polyakov loop. In this article, we use a smooth regularization procedure by introducing a form factor  $g_\Lambda(p)$  in the diverging zero-point energy. Our choice of  $g_\Lambda(p)$  is

$$g_\Lambda(p) = \frac{\Lambda^{2N}}{\Lambda^{2N} + (p_z^2 + 2|q_f e B|k)^N}, \quad (6)$$

we choose two values of  $N$ , namely  $N = 5$  and  $N = 7$ .

The potential term  $\mathcal{U}[P, \bar{P}, T]$  in Eq. (3) is built by hand in order to reproduce the pure gluonic lattice data [10]. Among several different potential choices [49], we adopt the following logarithmic form [9,10]:

$$\begin{aligned} \mathcal{U}[P, \bar{P}, T] = & T^4 \left\{ -\frac{a(T)}{2} \bar{P} P + b(T) \ln[1 - 6\bar{P} P \right. \\ & \left. + 4(\bar{P}^3 + P^3) - 3(\bar{P} P)^2 \right\}, \end{aligned} \quad (7)$$

with three model parameters (one of four is constrained by the Stefan-Boltzmann limit),

$$a(T) = a_0 + a_1 \left(\frac{T_0}{T}\right) + a_2 \left(\frac{T_0}{T}\right)^2, \quad b(T) = b_3 \left(\frac{T_0}{T}\right)^3. \quad (8)$$

The standard choice of the parameters reads [10]

$$\begin{aligned} a_0 = 3.51, & \quad a_1 = -2.47, \\ a_2 = 15.2, & \quad b_3 = -1.75. \end{aligned} \quad (9)$$

The parameter  $T_0$  in Eq. (7) sets the deconfinement scale in the pure gauge theory, i.e.  $T_c = 270$  MeV.

Before going ahead, we comment on the natural equality of  $\langle \bar{u} u \rangle$  and  $\langle \bar{d} d \rangle$  which arises in this model, even in the presence of an external magnetic field. In principle, one could expect the two condensates to be different when  $eB \neq 0$ , because  $\mathbf{B}$  couples in a different way to  $u$  and  $d$  quarks. However, because of the interaction in Eq. (1), the thermodynamic potential depends only on  $\langle \bar{u} u \rangle + \langle \bar{d} d \rangle$  even if  $\mathbf{B} \neq 0$ . Therefore, only the sum of the two condensates determines the ground state energy, the difference being undetermined. For this reason, we chose  $\langle \bar{d} d \rangle = \langle \bar{u} u \rangle$  at any value of temperature and magnetic field. We suppose that one way to remove this ambiguity is to introduce a different coupling constant for the anomalous and the non-anomalous interaction in Eq. (1). We leave this interesting investigation to a future work.

Following [42], in order to define the dressed Polyakov loop, we work in a finite Euclidean volume with temperature extension  $\beta = 1/T$ . We take twisted fermion boundary conditions along the compact temporal direction,

$$q(\mathbf{x}, \beta) = e^{-i\varphi} q(\mathbf{x}, 0), \quad \varphi \in [0, 2\pi], \quad (10)$$

while for spatial directions, the usual periodic boundary condition is taken. The canonical antiperiodic boundary condition for the quantization of fermions at finite temperature is obtained by taking  $\varphi = \pi$  in the previous equation. The dual quark condensate,  $\tilde{\Sigma}_n$ , is defined as

$$\tilde{\Sigma}_n(m, V) = \int_0^{2\pi} \frac{d\varphi}{2\pi} \frac{e^{-i\varphi n}}{V} \langle \bar{q}q \rangle_G, \quad (11)$$

where  $n$  is an integer. The expectation value  $\langle \cdot \rangle_G$  denotes the path integral over gauge field configurations. An important point is that in the computation of the expectation value, the twisted boundary conditions act only on the fermion determinant; the gauge fields are taken to be quantized with the canonical periodic boundary condition.

Using a lattice regularization, it has been shown in [42] that Eq. (11) can be expanded in terms of loops which wind  $n$  times along the compact time direction. In particular, the case  $n = 1$  is called the dressed Polyakov loop; it corresponds to a sum of loops winding just once along the time direction. These correspond to the thin Polyakov loop (the loop with shortest length) plus higher-order loops, the order being proportional to the length of the loop. Each higher-order loop is weighed by an inverse power of the quark mass. Because of the weight, in the infinite quark mass limit, only the thin Polyakov loop survives; for this reason, the dressed Polyakov loop can be viewed as a mathematical dressing of the thin loop by virtue of longer loops, the latter being more and more important as the quark mass tends to smaller values.

If we denote by  $z$  an element of the center of the color gauge group, then it is easy to show that  $\tilde{\Sigma}_n \rightarrow z^n \tilde{\Sigma}_n$ . It then follows that, under the center of the symmetry group  $Z_3$ , the dressed Polyakov loop is an order parameter for the center symmetry, with the same transformation rule of the thin Polyakov loop. Since the center symmetry is spontaneously broken in the deconfinement phase and restored in the confinement phase [7] (in the presence of dynamical quarks, it is only approximately restored), the dressed Polyakov loop can be regarded as an order parameter for the confinement-deconfinement transition as well.

For later convenience, we scale the definition of the dressed Polyakov loop in Eq. (11), and introduce

$$\begin{aligned} \Sigma_1 &= -2\pi g_\sigma \int_0^{2\pi} \frac{d\varphi}{2\pi} e^{-i\varphi} \langle \bar{q}q \rangle_G, \\ &= - \int_0^{2\pi} d\varphi e^{-i\varphi} \sigma(\varphi), \end{aligned} \quad (12)$$

where  $\sigma(\varphi)$  corresponds to the expectation value of the  $\sigma$  field computed, keeping twisted boundary conditions for fermions.

### III. NUMERICAL RESULTS

In this section, we show our results. The main goal to achieve numerically is the solution of the gap equations,

$$\frac{\partial \Omega}{\partial \sigma} = 0, \quad \frac{\partial \Omega}{\partial P} = 0. \quad (13)$$

This is done by using a globally convergent algorithm with backtrack [50]. From the very definition of the dressed Polyakov loop [42], the twisted boundary condition,

Eq. (10), must be imposed only on the Dirac operator; the ensemble averages have to be computed using the canonical antiperiodic boundary conditions. Therefore, we first compute the expectation value of the Polyakov loop and to the chiral condensate, taking  $\varphi = \pi$ . Then, in order to compute the dressed Polyakov loop using Eq. (12), we compute the  $\varphi$ -dependent chiral condensate using the first of Eq. (13), keeping the expectation value of the Polyakov loop fixed at its value at  $\varphi = \pi$  [21].

In this study, we report results obtained using the UV regulator specified in Eq. (6) with  $N = 5$  and  $N = 7$ . As expected, there is no qualitative difference among the pictures that the two regularization schemes lead to. As a consequence, concrete results are shown only for the case  $N = 5$ ; for what concerns the case  $N = 7$ , we collect the pseudocritical temperatures in Table II. We have also checked that the results are qualitatively unchanged if we use a hard cutoff scheme instead of the smooth UV regulator. The parameter set for both cases is specified in Table I. In the case  $N = 5$ , they are obtained by the requirements that the vacuum pion mass is  $m_\pi = 139$  MeV, the pion decay constant  $f_\pi = 92.4$  MeV, and the vacuum chiral condensate  $\langle \bar{u}u \rangle \approx (-241 \text{ MeV})^3$ . In this case, the chiral and deconfinement pseudocritical temperatures at zero magnetic field are  $T_0^X = T_0^P = 175$  MeV. Similarly, for the case  $N = 7$ , the chiral and deconfinement pseudocritical temperatures at zero magnetic field are  $T_0^X = 176$  MeV and  $T_0^P = 175$  MeV, respectively; the zero temperature chiral condensate at zero magnetic field strength is fixed to  $\langle \bar{u}u \rangle \approx (-246 \text{ MeV})^3$ .

We remark that the main effect of the eight-quark interaction in Eq. (1) is to lower the pseudocritical temperature of the crossovers. This has been already discussed several times in the literature [45,46], in the context of both the NJL and the P-NJL models. Therefore, it is not necessary to discuss it further here, while at the same time we prefer to stress the results that have not yet been discussed.

In order to identify the pseudocritical temperatures, we have defined the *effective susceptibilities* as

$$\chi_A = (m_\pi)^g \left| \frac{dA}{dT} \right|, \quad A = \sigma, P, \Sigma_1. \quad (14)$$

Strictly speaking, the quantities defined in the previous equation are not true susceptibilities. Nevertheless, they allow us to represent faithfully the pseudocritical region, that is, the range in temperature in which the various crossovers take place. Therefore, for our purposes it is enough to compute these quantities. In Eq. (14), the

TABLE I. Parameters of the model for the two choices of the UV regulator.

	$\Lambda$ (MeV)	$m_0$ (MeV)	$g_\sigma$ (MeV) <sup>-2</sup>	$g_8$ (MeV) <sup>-8</sup>
$N = 5$	588.657	5.61	$5 \times 10^{-6}$	$6 \times 10^{-22}$
$N = 7$	603.475	5.61	$4.92 \times 10^{-6}$	$6.8 \times 10^{-22}$

TABLE II. Coefficients of the fit function defined in Eq. (15).

	$a$	$\alpha$	$T_0$ (MeV)	$\varepsilon$
$T_\chi, N = 5$	$2.4 \times 10^{-3}$	1.85	175	0.21
$T_P, N = 5$	$2.1 \times 10^{-3}$	1.41	175	0.08
$T_\chi, N = 7$	$7.8 \times 10^{-3}$	1.29	176	0.19
$T_P, N = 7$	$3.9 \times 10^{-3}$	1.08	176	0.01

appropriate power of  $m_\pi$  is introduced just for a matter of convenience, in order to have a dimensionless quantity; therefore,  $g = 0$  if  $A = \sigma, \Sigma_1$ , and  $g = 1$  if  $A = P$ .

### A. Condensates and dressed Polyakov loop

From now on, we fix  $N = 5$  unless specified. The results for this case are collected in the form of three-dimensional plots in Fig. 1 (for the case  $N = 7$ , the plots do not differ qualitatively). In the left panel, we plot the chiral condensate  $\langle \bar{u}u \rangle^{1/3}$ , the expectation value of the Polyakov loop, and the dressed Polyakov loop  $\Sigma_1$  as functions of temperature and magnetic field. In the right panel, we show the contour plots of the raw data of the effective susceptibilities. The lighter the color, the higher the susceptibility. In the contour plots, the vertical axes correspond to temperature (measured in MeV); the horizontal axes represent the magnetic field  $eB/m_\pi^2$ .

We slice the three-dimensional plots in Fig. 1 at fixed value of the magnetic field strength and show the results in Fig. 2, where we plot the chiral condensate  $S = |\langle \bar{u}u \rangle|^{1/3}$  (upper panel), the Polyakov loop (middle panel), and  $\Sigma_1$  (lower panel) as a function of temperature, for several values of the applied magnetic field strength, measured in units of  $m_\pi^2$ . In the right panel, we plot fits of the effective susceptibilities in the critical regions, as a function of temperature. The fits are obtained from the raw data, using Breit-Wigner-like fitting functions. The details of the fitting procedure are not relevant for the present discussion. For graphical reasons, in Fig. 1 we plot the chiral condensate with its sign; on the other hand, in Fig. 2 we take the absolute value of this quantity.

The qualitative behavior of the chiral condensate, and of the Polyakov loop as well, are similar to that found in a previous study within the P-NJL model in the chiral limit [35]. Quantitatively, the main difference with the case of the chiral limit is that in the latter, the chiral symmetry restoration at large temperature is a true second-order phase transition (in other model calculations, it has been reported that the phase transition might become of the first order at very large magnetic field strengths [34]). On the other hand, in the case under investigation, chiral symmetry is always broken explicitly because of the bare quark masses; as a consequence, the second-order phase transition is replaced by a smooth crossover.

Another interesting aspect, observed also in the chiral limit [35], is that the Polyakov loop crossover temperature is less sensitive to the strength of the magnetic field than

the same quantity computed for the chiral condensate. It is useful, for illustrative purposes, to quantify the net shift of the pseudocritical temperatures for the largest value of magnetic field we have studied,  $eB = 19m_\pi^2$ . In this case, if we take  $N = 5$  (the results are similar for  $N = 7$ ), then the two crossovers occur simultaneously at  $eB = 0$ , at the temperature  $T_0^\chi = T_0^P = 175$  MeV; for  $eB = 19m_\pi^2$ , we find  $T_\chi = 219$  MeV and  $T_P = 190$  MeV. Therefore, the chiral crossover is shifted approximately by 25.1%, to be compared with the more modest shift of the Polyakov loop crossover, which is  $\approx 8.6\%$ .

The split of the two critical temperatures at so large a value of magnetic field strength is only 15%; on the lattice, no split is observed [26], and a modest increase of the critical temperature is measured. Therefore, we are in partial agreement with the lattice results, in the sense that the raising of the critical lines is observed also in our model calculation; for what concerns the split of the two crossovers, we can take our  $\mathcal{O}(10\%)$  split as a consequence of the crudeness of the model at hand. On the lattice, the smaller pion mass used is of the order of 200 MeV [26]. We have verified that our qualitative picture is unchanged if we artificially increase the vacuum pion mass up to this value. In passing, we notice that, using a running coupling (as in [51]) but at the same time adding two further free parameters in the model, we expect a better agreement with the lattice. The reason is that in [51], the coupling  $g_\sigma$  is a function of the Polyakov loop, and it decreases as  $P$  is increased. As a consequence, near the Polyakov loop crossover temperature, the strength of the interaction is lowered, and a partial suppression of the chiral condensate is expected. Quantitatively, it is not clear *a priori* if the suppression is enough to rejoin the two crossovers; only a detailed numerical study can give the answer. We leave this important investigation to a future study.

The tiny decoupling of the two crossovers found within the P-NJL model, both in the chiral limit [35] and in the case of physical pion mass considered here, is observed also within the Polyakov quark-meson model [36]; when in the latter, the zero-point energy is considered (if the vacuum energy is subtracted, then the Polyakov loop and the chiral crossovers occur always simultaneously, but the pseudocritical temperature is a decreasing function of  $eB$ , which seems in disagreement with the recent lattice results [26]; see also [52] for a recent discussion of the role of the vacuum energy within the quark-meson model). Since the Polyakov loop is coupled to quarks in the same manner both in the P-NJL and in the PQM model, the tiny split of the two crossovers as  $eB$  is increased does not appear as an artifact of the P-NJL model; instead, it seems to be a consequence of the link among the chiral condensate and the Polyakov loop, which is common in the two kinds of models.

In the lower panels of Figs. 1 and 2, we plot the dressed Polyakov loop as a function of temperature, for several

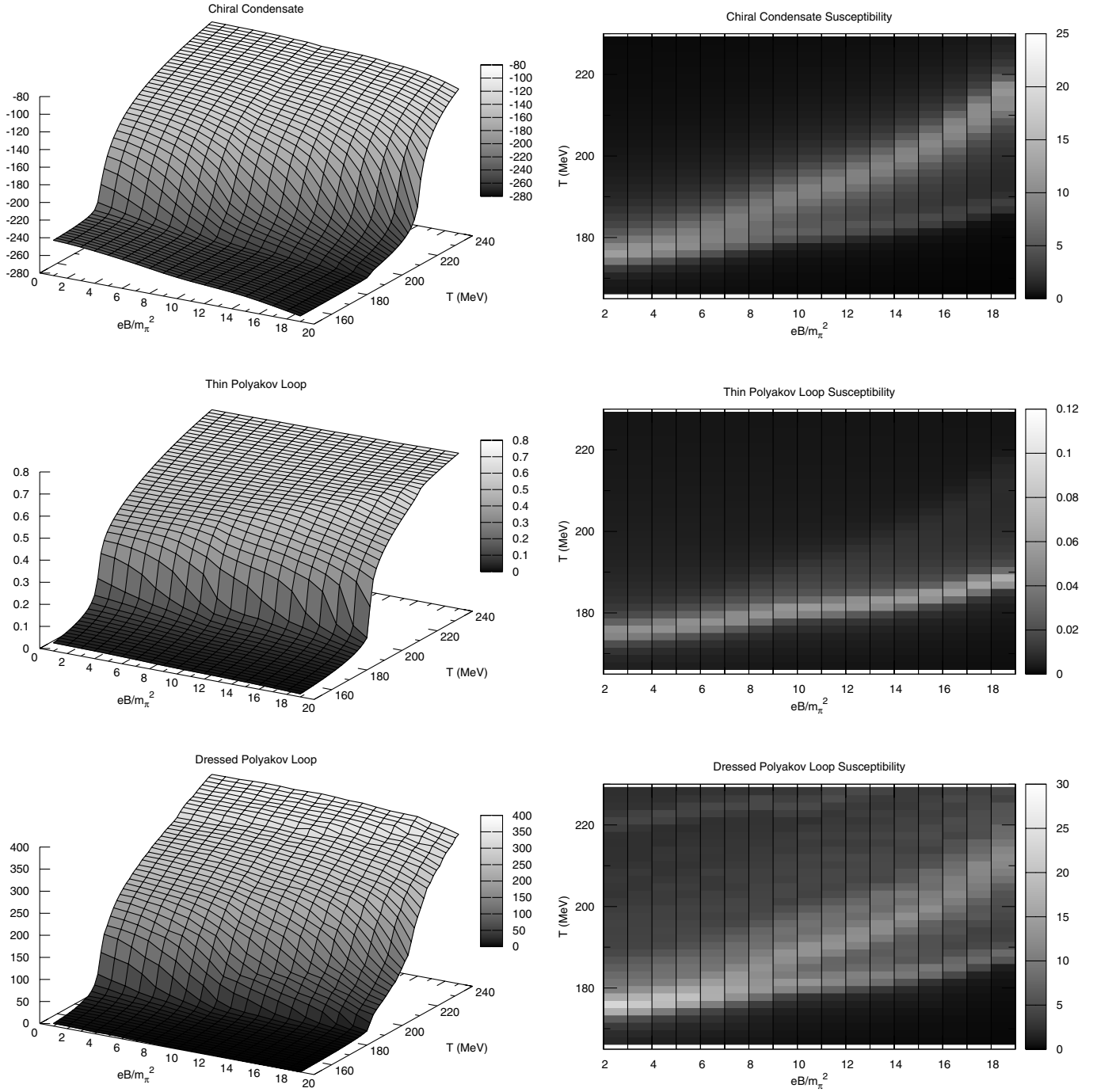


FIG. 1 (color online). *Left panel.* Chiral condensate, Polyakov loop, and dressed Polyakov loop as a function of temperature and magnetic field, for the case  $N = 5$ . *Right panel.* Contour plots of the raw data of the effective susceptibilities. The lighter the color, the higher the susceptibility. Vertical axes correspond to temperature (in MeV); horizontal axes represent magnetic field  $eB/m_\pi^2$ . For the dressed Polyakov loop susceptibility, the bifurcation of the critical region is evident.

values of  $eB$ . Our definition, Eq. (12), differs from the canonical one [42] for an overall factor, which gives mass dimension one to our  $\Sigma_1$ . For small values of  $eB/m_\pi^2$ , the behavior of  $\Sigma_1$  as temperature is increased is qualitatively similar to that at  $eB = 0$ , which has been discussed within effective models in [21,44]. In particular, the dressed Polyakov loop is very small for temperatures below the

pseudocritical temperature of the simultaneous crossover. Then, it experiences a crossover in correspondence of the simultaneous Polyakov loop and chiral condensate crossovers. It eventually saturates at very large temperature (for example, in [21], the saturation occurs at a temperature of the order of 0.4 GeV, in agreement with the results of [44]). However, we do not push up our numerical calculation to

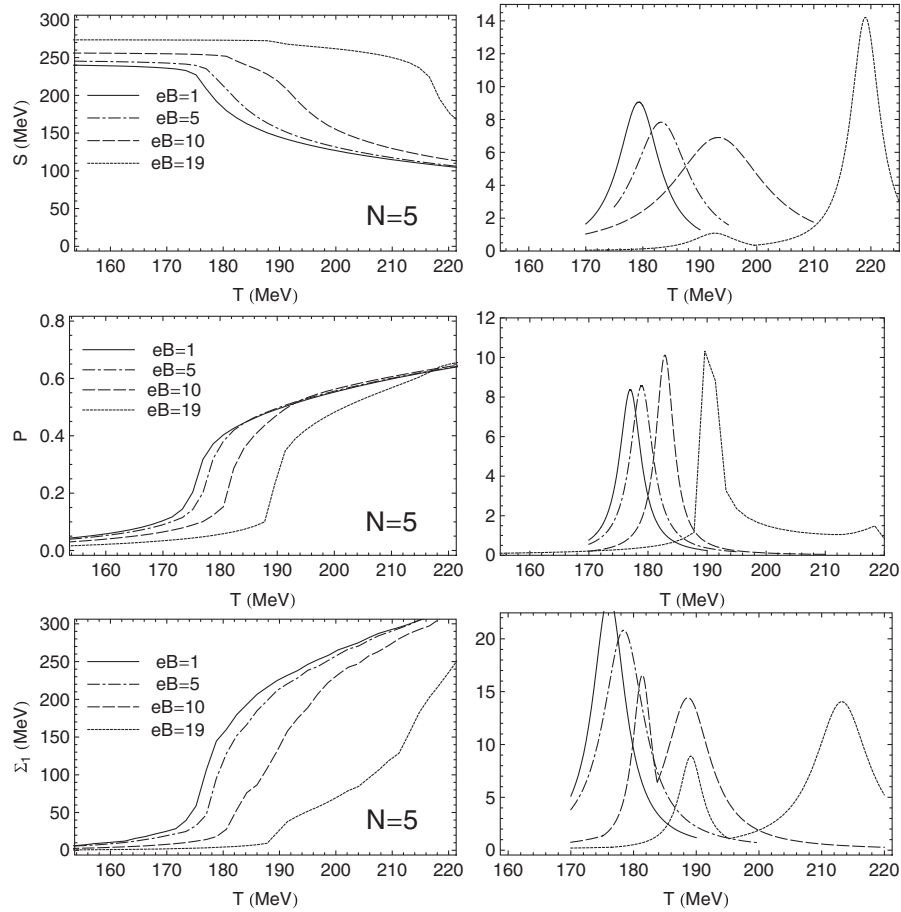


FIG. 2. *Left panel.* Chiral condensate  $S = |\langle \bar{u}u \rangle|^{1/3}$  (upper panel), Polyakov loop (middle panel), and  $\Sigma_1$  (lower panel) as a function of temperature, for several values of the applied magnetic field strength, measured in units of  $m_\pi^2$ . In the figures,  $N = 5$  corresponds to the order of the UV regulator in Eq. (6). *Right panel.* Effective susceptibilities, defined in Eq. (14), as a function of temperature, for several values of  $eB$ . Conventions for lines are the same as in the left panel.

such a high temperature, because we expect that the effective model in that case is well beyond its range of validity.

As we increase the value of  $eB$ , as noticed previously, we observe a tiny splitting of the chiral and the Polyakov loop crossovers. Correspondingly, the qualitative behavior of the dressed Polyakov loop changes dramatically: the range of temperature in which the  $\Sigma_1$  crossover takes place is enlarged, if compared to the thin temperature interval in which the crossover takes place at the lowest value of  $eB$  (compare the solid and the dotted lines in Fig. 2, as well as the lower panel of Fig. 1).

The effective susceptibility,  $d\Sigma_1/dT$ , plotted in the lower right panel of Fig. 2, is qualitatively very interesting. We observe a double-peak structure, which we interpret as the fact that the dressed Polyakov loop is capable of feeling (and, hence, describing) both the crossovers. If we were to interpret  $\Sigma_1$  as the order parameter for deconfinement, and the temperature with the largest susceptibility with the crossover pseudocritical temperature, then we would obtain almost simultaneous crossover even for very large magnetic field. If this were the case, then the Polyakov

loop computed within the P-NJL model should be interpreted only as an indicator of statistical confinement, and the deconfinement would be described by  $\Sigma_1$ . Of course, this picture would not contradict the well-established picture at zero magnetic field [9–11]. Indeed, in the case of small  $eB$ , we find simultaneous crossover of chiral condensate, the Polyakov loop, and the dressed Polyakov loop. In the latter case, it would just be a matter of taste which quantity one would use to identify the deconfinement crossover. Even if it is tempting to give this kind of interpretation, which would lead to simultaneous crossover also at finite  $eB$ , it is very hard to accept it without more convincing microscopic arguments. Therefore, in the prosecution of this work, we prefer to associate the deconfinement crossover to that of the Polyakov loop. Nevertheless, the dressed Polyakov loop is a new quantity which is interesting to compute. In particular, the double-peak structure in the  $\Sigma_1$  effective susceptibility, which is produced if the magnetic field is strong enough, offers the evidence that the dressed Polyakov loop is intimately related to both chiral condensate and (thin) Polyakov

loop, and it is capable of capturing both the crossovers. The bifurcation of the dressed Polyakov loop susceptibility in the lower right panel of Fig. 1 is impressive.

### B. Phase diagram in the $eB$ - $T$ plane

In Fig. 3, we collect our results on the pseudocritical temperatures for chiral and Polyakov loop crossovers, in the form of phase diagrams in the  $eB$ - $T$  plane. The dashed line denotes the Polyakov loop crossover, and the dot-dashed line corresponds to the chiral crossover. The shaded area is the region in the  $eB$ - $T$  plane in which quark matter is not statistically confined, but chiral symmetry is still broken by the chiral condensate. Temperatures on the vertical axes are measured in units of the pseudocritical temperature at zero field, which is  $T_0 = 175$  MeV. We fit our data on the pseudocritical temperatures by the law

$$\frac{T_c^A}{T_0} = 1 + a \left( \frac{eB}{T_0} \right)^\alpha, \quad (15)$$

where  $A = \sigma, P$ . Numerical values of the coefficients in Eq. (15) for the various observables are collected in Table II. As an estimator of the accuracy of the various fits, we report in Table II the percentage error defined as

$$\varepsilon = 100 \times \sum_i \left( \frac{f_A(x_i) - y_i}{y_i} \right)^2, \quad (16)$$

where the sum runs over the data,  $(x_i, y_i)$  corresponds to a couple in the set of the data  $(eB, T_A)$ , and  $f_A(x_i)$  denotes the numerical value of the fit function evaluated at the data  $eB$ .

The picture discussed in the previous section is made clear by the phase diagrams in Fig. 3. We measure an

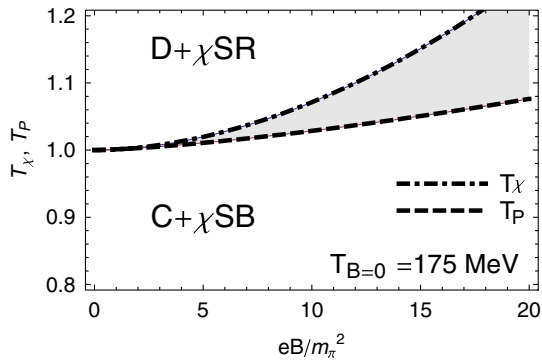


FIG. 3 (color online). Phase diagram of the P-NJL model in magnetic field. Dashed line denotes the Polyakov loop crossover; dot-dashed line corresponds to the chiral crossover. The shaded area is the region, in the  $eB$ - $T$  plane, in which quark matter is not statistically confined, but chiral symmetry is still broken by the chiral condensate. Temperatures on the vertical axes are measured in units of the pseudocritical temperature at zero field, which is  $T_0 = 175$  MeV. The analytic form of the lines corresponding to  $T_P$  and  $T_\chi$  is specified by Eq. (15). The UV regulator is that corresponding to  $N = 5$ .

increase of both deconfinement and chiral crossovers; the tiny split of the two critical temperatures is of the order of 10% for the largest value of the magnetic field strength considered here.

It is instructive to compare our results with those obtained in a different model. The shape of the phase diagram drawn in Fig. 3 is similar to that drawn by the Polyakov extended quark-meson model; see, e.g., Fig. 13 of [36]. In that reference, an interpretation of the split in terms of the interplay among vacuum and thermal contributions is given. We totally agree with those arguments, which are reproduced within the P-NJL model as well, as the final results on critical temperatures show. In the case of the quark-meson model, however, the picture can change even qualitatively, depending on the fate of vacuum energy contribution. If they are not included, then a simultaneous first-order transition is observed at every value of  $eB$  (if  $eB$  is very small, the transition is a smooth crossover), and the deconfinement temperature as a function of the magnetic field strength *decreases*. This picture confirms the scenario anticipated in a previous work [34]. In the case of the P-NJL model, we cannot reproduce the latter scenario because of a technical reason: indeed, in our case, the vacuum contribution cannot be subtracted (as a matter of fact, we do not have a further effective potential term at zero temperature, which leads to spontaneous breaking of chiral symmetry when vacuum quark contributions are subtracted). Therefore, we limit ourselves only to a comparison with the quark-meson model with vacuum contributions taken into account.

## IV. CONCLUSIONS

We have computed, for the first time in the literature, the dressed Polyakov loop for hot quark matter in external magnetic field. To compute the finite temperature effective potential in magnetic field, we have used the Polyakov extended Nambu–Jona-Lasinio model, with a logarithm-effective action for the Polyakov loop. In the quark sector, we have used both a four-quark and an eight-quark interaction. Bare quark masses are fixed to reproduce the physical value of the vacuum pion mass. This model allows us to treat self-consistently both chiral symmetry breaking and (statistical) confinement. We improve the previous work in [35] in three ways: we set the vacuum pion mass to its physical value; we introduce the eight-quark interaction; finally, we compute the dressed Polyakov loop.

Our results on the dressed Polyakov loop,  $\Sigma_1$ , in magnetic field show that this quantity is capable of describing both Polyakov loop and chiral crossovers. This is resumed in the double-peak structure of the effective susceptibility  $d\Sigma_1/dT$ ; see Figs. 1 and 3.

The results of the pseudocritical temperatures as a function of  $eB$  are resumed in the phase diagrams in Fig. 3. These results were anticipated in a previous work [35] in which only the chiral limit was considered, and the

eight-quark interaction was neglected. Our results agree qualitatively with those of [36], in which a quark-meson model coupled to the Polyakov loop is considered.

As an improvement of our results, it would be interesting to consider the effects of nonlocality [24]. In that case, however, the computation of the fermion spectrum in the magnetic field is not trivial because of the nonlocal structure of the action. Another interesting possibility is the use of Monte Carlo methods to compute the P-NJL partition function in magnetic field, going beyond the saddle approximation. Encouraging results along this research line in the context of the P-NJL model have been reported in [53]. Therefore, it might be interesting to extend the computation of [53] to the case of quarks in external magnetic field. Even more, we expect that the running coupling introduced by the Kyushu group [51] would help (at least

partly) to get closer crossovers in magnetic field. A numerical investigation of this subject is left to a future study. Finally, the extension of our calculation to finite quark chemical potential, and to quark matter in external chromomagnetic fields, the latter being motivated by lattice results [29,30], would deserve further attention.

## ACKNOWLEDGMENTS

We acknowledge correspondence with M. Huang and S. Nicotri, and, in particular, with M. d’Elia. Moreover, we acknowledge stimulating discussions with L. Campanelli and K. Fukushima. The work of M. R. is supported by JSPS under the contract number P09028. The numerical calculations were carried out on Altix3700 BX2 at YITP in Kyoto University.

- 
- [1] P. de Forcrand and O. Philipsen, *J. High Energy Phys.* **01** (2007) 077; **11** (2008) 012; *Proc. Sci., LATTICE2008* (2008) 208.
- [2] Y. Aoki, Z. Fodor, S. D. Katz, and K. K. Szabo, *Phys. Lett. B* **643**, 46 (2006); Y. Aoki, S. Borsanyi, S. Durr, Z. Fodor, S. D. Katz, S. Krieg, and K. K. Szabo, *J. High Energy Phys.* **06** (2009) 088.
- [3] A. Bazavov *et al.*, *Phys. Rev. D* **80**, 014504 (2009).
- [4] M. Cheng *et al.*, *Phys. Rev. D* **81**, 054510 (2010).
- [5] Y. Nambu and G. Jona-Lasinio, *Phys. Rev.* **122**, 345 (1961); **124**, 246 (1961).
- [6] U. Vogl and W. Weise, *Prog. Part. Nucl. Phys.* **27**, 195 (1991); S. P. Klevansky, *Rev. Mod. Phys.* **64**, 649 (1992); T. Hatsuda and T. Kunihiro, *Phys. Rep.* **247**, 221 (1994); M. Buballa, *Phys. Rep.* **407**, 205 (2005).
- [7] A. M. Polyakov, *Phys. Lett.* **72B**, 477 (1978); L. Susskind, *Phys. Rev. D* **20**, 2610 (1979); B. Svetitsky and L. G. Yaffe, *Nucl. Phys.* **B210**, 423 (1982); B. Svetitsky, *Phys. Rep.* **132**, 1 (1986).
- [8] P. N. Meisinger and M. C. Ogilvie, *Phys. Lett. B* **379**, 163 (1996).
- [9] K. Fukushima, *Phys. Lett. B* **591**, 277 (2004).
- [10] C. Ratti, M. A. Thaler, and W. Weise, *Phys. Rev. D* **73**, 014019 (2006).
- [11] S. Roessner, C. Ratti, and W. Weise, *Phys. Rev. D* **75**, 034007 (2007).
- [12] E. Megias, E. Ruiz Arriola, and L. L. Salcedo, *Phys. Rev. D* **74**, 114014 (2006); *Eur. Phys. J. A* **31**, 553 (2007).
- [13] C. Sasaki, B. Friman, and K. Redlich, *Phys. Rev. D* **75**, 074013 (2007).
- [14] S. K. Ghosh, T. K. Mukherjee, M. G. Mustafa, and R. Ray, *Phys. Rev. D* **77**, 094024 (2008).
- [15] K. Fukushima, *Phys. Rev. D* **77**, 114028 (2008); **78**, 039902 (2008); M. Ciminale, R. Gatto, N. D. Ippolito, G. Nardulli, and M. Ruggieri, *Phys. Rev. D* **77**, 054023 (2008); W. J. Fu, Z. Zhang, and Y. x. Liu, *Phys. Rev. D* **77**, 014006 (2008); T. Hell, S. Rossner, M. Cristoforetti, and W. Weise, *Phys. Rev. D* **81**, 074034 (2010).
- [16] L. McLerran and R. D. Pisarski, *Nucl. Phys.* **A796**, 83 (2007).
- [17] H. Abuki, R. Anglani, R. Gatto, G. Nardulli, and M. Ruggieri, *Phys. Rev. D* **78**, 034034 (2008).
- [18] T. Kahara and K. Tuominen, *arXiv:1006.3931*.
- [19] Y. Sakai, K. Kashiwa, H. Kouno, and M. Yahiro, *Phys. Rev. D* **77**, 051901 (2008); **78**, 036001 (2008).
- [20] Y. Sakai, K. Kashiwa, H. Kouno, M. Matsuzaki, and M. Yahiro, *Phys. Rev. D* **79**, 096001 (2009).
- [21] K. Kashiwa, H. Kouno, and M. Yahiro, *Phys. Rev. D* **80**, 117901 (2009).
- [22] H. Abuki, M. Ciminale, R. Gatto, N. D. Ippolito, G. Nardulli, and M. Ruggieri, *Phys. Rev. D* **78**, 014002 (2008); H. Abuki, M. Ciminale, R. Gatto, and M. Ruggieri, *Phys. Rev. D* **79**, 034021 (2009).
- [23] Y. Sakai, T. Sasaki, H. Kouno, and M. Yahiro, *arXiv:1005.0910*.
- [24] T. Hell, S. Roessner, M. Cristoforetti, and W. Weise, *Phys. Rev. D* **79**, 014022 (2009).
- [25] K. Kashiwa, H. Kouno, M. Matsuzaki, and M. Yahiro, *Phys. Lett. B* **662**, 26 (2008).
- [26] M. D’Elia, S. Mukherjee, and F. Sanfilippo, *Phys. Rev. D* **82**, 051501 (2010).
- [27] P. V. Buividovich, M. N. Chernodub, E. V. Luschevskaya, and M. I. Polikarpov, *Phys. Rev. D* **81**, 036007 (2010).
- [28] P. V. Buividovich, M. N. Chernodub, E. V. Luschevskaya, and M. I. Polikarpov, *Phys. Lett. B* **682**, 484 (2010).
- [29] P. Cea and L. Cosmai, *J. High Energy Phys.* **02** (2003) 031; **08** (2005) 079.
- [30] P. Cea, L. Cosmai, and M. D’Elia, *J. High Energy Phys.* **12** (2007) 097.
- [31] S. P. Klevansky and R. H. Lemmer, *Phys. Rev. D* **39**, 3478 (1989); H. Suganuma and T. Tatsumi, *Ann. Phys. (N.Y.)* **208**, 470 (1991); I. A. Shushpanov and A. V. Smilga, *Phys. Lett. B* **402**, 351 (1997); D. N. Kabat, K. M. Lee, and E. J.

- Weinberg, *Phys. Rev. D* **66**, 014004 (2002); T. Inagaki, D. Kimura, and T. Murata, *Prog. Theor. Phys.* **111**, 371 (2004); T.D. Cohen, D.A. McGady, and E.S. Werbos, *Phys. Rev. C* **76**, 055201 (2007); K. Fukushima and H.J. Warringa, *Phys. Rev. Lett.* **100**, 032007 (2008); J.L. Noronha and I.A. Shovkovy, *Phys. Rev. D* **76**, 105030 (2007).
- [32] V.P. Gusynin, V.A. Miransky, and I.A. Shovkovy, *Nucl. Phys.* **B462**, 249 (1996); **B563**, 361 (1999); G.W. Semenoff, I.A. Shovkovy, and L.C.R. Wijewardhana, *Phys. Rev. D* **60**, 105024 (1999); V.A. Miransky and I.A. Shovkovy, *Phys. Rev. D* **66**, 045006 (2002).
- [33] K.G. Klimenko, *Teor. Mat. Fiz.* **89**, 211 (1991); [*Theor. Math. Phys.* **89**, 1161 (1991)]; *Z. Phys. C* **54**, 323 (1992); *Teor. Mat. Fiz.* **90**, 1 (1992); [*Theor. Math. Phys.* **90**, 1 (1992)].
- [34] N.O. Agasian and S.M. Fedorov, *Phys. Lett. B* **663**, 445 (2008); E.S. Fraga and A.J. Mizher, *Phys. Rev. D* **78**, 025016 (2008).
- [35] K. Fukushima, M. Ruggieri, and R. Gatto, *Phys. Rev. D* **81**, 114031 (2010).
- [36] A.J. Mizher, M.N. Chernodub, and E.S. Fraga, [arXiv:1004.2712](https://arxiv.org/abs/1004.2712).
- [37] L. Campanelli and M. Ruggieri, *Phys. Rev. D* **80**, 034014 (2009).
- [38] D.E. Kharzeev, L.D. McLerran, and H.J. Warringa, *Nucl. Phys.* **A803**, 227 (2008).
- [39] V. Skokov, A.Y. Illarionov, and V. Toneev, *Int. J. Mod. Phys. A* **24**, 5925 (2009).
- [40] P.V. Buividovich, M.N. Chernodub, E.V. Luschevskaya, and M.I. Polikarpov, *Phys. Rev. D* **80**, 054503 (2009); M. Abramczyk, T. Blum, G. Petropoulos, and R. Zhou, [arXiv:0911.1348](https://arxiv.org/abs/0911.1348).
- [41] K. Fukushima, D.E. Kharzeev, and H.J. Warringa, *Phys. Rev. D* **78**, 074033 (2008).
- [42] E. Bilgici, F. Bruckmann, C. Gattlinger, and C. Hagen, *Phys. Rev. D* **77**, 094007 (2008).
- [43] C.S. Fischer, *Phys. Rev. Lett.* **103**, 052003 (2009); C.S. Fischer and J.A. Mueller, *Phys. Rev. D* **80**, 074029 (2009); C.S. Fischer, A. Maas, and J.A. Mueller, [arXiv:1003.1960](https://arxiv.org/abs/1003.1960).
- [44] T.K. Mukherjee, H. Chen, and M. Huang, *Phys. Rev. D* **82**, 034015 (2010).
- [45] A.A. Osipov, B. Hiller, J. Moreira, A.H. Blin, and J. da Providencia, *Phys. Lett. B* **646**, 91 (2007).
- [46] K. Kashiwa, H. Kouno, T. Sakaguchi, M. Matsuzaki, and M. Yahiro, *Phys. Lett. B* **647**, 446 (2007).
- [47] A.A. Osipov, B. Hiller, and J. da Providencia, *Phys. Lett. B* **634**, 48 (2006).
- [48] A.A. Osipov, B. Hiller, A.H. Blin, and J. da Providencia, *Phys. Lett. B* **650**, 262 (2007).
- [49] B.J. Schaefer, M. Wagner, and J. Wambach, *Phys. Rev. D* **81**, 074013 (2010).
- [50] W. Press, S.A. Teukolsky, W.T. Vetterling, and B.P. Flannery, *Numerical Recipes: The Art of Scientific Computing* (Cambridge University Press, Cambridge, England, 2007), 3rd ed..
- [51] Y. Sakai, T. Sasaki, H. Kouno, and M. Yahiro, [arXiv:1006.3648](https://arxiv.org/abs/1006.3648).
- [52] V. Skokov, B. Friman, E. Nakano, K. Redlich, and B.J. Schaefer, *Phys. Rev. D* **82**, 034029 (2010).
- [53] M. Cristoforetti, T. Hell, B. Klein, and W. Weise, *Phys. Rev. D* **81**, 114017, (2010).